

Split-Ring Resonator Arrays for Electromagnetic Energy Harvesting

Thamer S. Almomneef and Omar M. Ramahi*

Abstract—By virtue of their ability to resonate at a wavelength much larger than the maximum dimension, Split-Ring Resonator (SRR) cells can be densely stacked to create energy harvesting arrays having per-unit-area power efficiency higher than a single SRR cell. While the concept of using metamaterial particles for electromagnetic energy harvesting had been demonstrated in our earlier work, the overall efficiency of an SRR array in comparison to classical antenna arrays is fundamental to the viability of this technology. In this work, we focus on a comparative study based on numerical full-wave simulations where an array of SRRs is compared to an array of microstrip antennas. We show that an SRR array can provide significant enhancement in power efficiency and bandwidth in comparison to the classical microstrip patch antenna. Experimental validation is provided showing SRR arrays can provide significant energy-absorption enhancement.

1. INTRODUCTION

It could be argued that Wireless Power Transfer (WPT) dates back to 1888 when Heinrich Hertz demonstrated electromagnetic wave propagation in free space [1]. Hertz used half-wavelength dipoles operating at 500 MHz along with parabolic reflectors for transmitting and receiving electromagnetic energy. At the turn of the 20th century, experiments on the concept of WPT were conducted by Nickola Tesla who built a gigantic coil resonating at 150 kHz. The coil was then excited with low frequency power source of 300 kW. Tesla's coil succeeded in lighting 200 light bulbs placed 42 km away [2]. Tesla's work intrigued many researchers in Japan [3] and the US [4]. It was not until the 1950s that the WPT was revisited with the development of high power microwave tubes by the Raytheon Company. These tubes were considered essential for transmitting efficient high power at GHz frequencies. In 1963, Brown and his colleagues demonstrated the first complete and efficient WPT system. A horn antenna operating at 2.45 GHz with power levels of 400 W was used to transmit microwave energy. At the receiving end, a diagonal horn antenna was used to collect the microwave energy, which was then converted back to DC by means of thermionic diodes. Conversion efficiency of only 50% was realized [1, 5].

In 1968, Glasser proposed a concept to use rectennas to harvest energy from space in what was termed as Space Solar Power (SSP) [6]. In SSP, solar energy is converted to electricity using arrays of solar cells placed 22,300 miles above the equator. Then the collected power is converted to microwaves and transmitted to a receiver site located on earth using a highly directive antenna. Large rectenna arrays would then receive the microwave energy and convert it to electricity [7]. Since the total efficiency of the WPT system depends significantly on the receiving system, commonly referred to as the rectenna system, research on this subject has focused on developing various rectenna systems that yield higher AC to DC conversion efficiencies. In 1977, Brown developed a 2.45 GHz rectenna system that reached a conversion efficiency of 90.6% [8]. Both the dipole antenna and the transmission lines used in this system were made out of aluminum bars. The microwave power collected by the antenna was converted

Received 25 January 2015, Accepted 6 March 2015, Scheduled 14 March 2015

* Corresponding author: Omar M. Ramahi (oramahi@uwaterloo.ca).

The authors are with the School of Electrical and Computer Engineering, University of Waterloo, Waterloo, Ontario N2L 3G1, Canada.

to DC using a GaAs-Pt Schottky barrier diode. The conversion efficiency of this rectenna system was then recognized as having one of the highest efficiencies ever recorded [9]. In 1985, Brown and Triner developed a rectenna system using printed thin film technology. The rectenna system was designed to operate at 2.45 GHz and was able to achieve 85% conversion efficiency while 10 times lighter than the previously developed rectennas [10]. Since then, most rectenna systems have been made using photolithographic etching techniques to reduce cost and weight [5]. While Brown's work is pioneering in many respects, he never provided explicit details in his published works on how the conversion efficiency was calculated.

In most of the aforementioned works, rectenna systems have been designed to operate at around 2.45 GHz. In 1991 a 35 GHz rectenna was developed by ARCO Power Technologies with a total conversion efficiency of 72% [11]. A low atmospheric absorption was the primary advantage of operating in the vicinity of 35 GHz but required the use of expensive and relatively less efficient components [9]. The first C band rectenna array was designed to operate at 5.87 GHz. This rectenna array was comprised of 1000 dipole antennas feeding rectifier circuits with silicon quad-bridge Schottky diodes having high reverse voltage. The diodes had the advantage of higher power-handling capabilities than those of the previously used GaAs diodes [12], thus achieving conversion efficiencies exceeding 80%.

Recent research in rectenna systems focused on improving different aspects of the system to suit the targeted applications. Generally, linearly-polarized microstrip antennas were used to capture microwave energy; however in [13] circular polarized antennas were used. Such polarization eliminates polarization mismatch losses and ensures that the voltage across the load remains relatively constant irrespective of any rotations of the system [14]. Since the amount of power harvested by one element collector is not sufficient for some applications, an array of antennas is usually used to increase the DC power supplied to the load as in [13, 15]. A 64-element spiral antenna array was used in [16] with the advantage of harvesting energy over a broad band covering frequencies from 2–18 GHz.

In all previous reported electromagnetic energy harvesting systems, especially the rectenna part of the system, conventional antennas were used. The highest emphasis in previous works was on maximizing the rf to dc conversion efficiency. In fact, the efficiency of the receiving antenna was not considered as the focus of earlier works. Power harvesting is constrained by real estate in a manner similar to harvesting solar energy using solar panels. Therefore, the size of the antenna and the number of antennas that can be grouped on a specific platform matter significantly to the overall efficiency of the energy harvesting system. Most recently, attention was given to miniaturization of antennas to achieve higher reception efficiency with the size of the platform constraints in mind.

In an earlier work [17], we introduced metamaterial for electromagnetic energy harvesting. In [17], we demonstrated through a simple experiment that a single metamaterial cell is capable of receiving power. The distinctive appeal of metamaterial cells is their small physical footprint which allows dense stacking creating what is typically referred to as metamaterial. The work in [17] demonstrated the reception of AC power by the metamaterial cell and demonstrated through numerical simulation that a densely packed two-dimensional array of SRRs can achieve energy harvesting efficiency of more than 75%. Also in [17], we made the obvious conclusion that AC power can be converted to DC power using classical matching and rectifying techniques such as [18–22]. In [23], an experimental demonstration of the ability of 5×1 split ring resonators to convert the harvested energy into DC was provided. Although the work in [23] demonstrated a 36% efficiency of microwave to DC power conversion, the five antennas used were indeed split ring resonators but their dimension and separation relative to the wavelength precludes the five elements from acting or be considered as a metamaterial. For an ensemble of cells to comprise a metamaterial, two conditions need to hold. The first is the largest dimension of each cell to be much smaller than the free-space wavelength; and second, the separation between the cells need to be much smaller than the free-space wavelength. The criterion for the separation of the cells is more relevant to engineered media with desired dispersive characteristics as homogenization and the subsequent concept of relative dielectric permittivity (or relative magnetic permeability) would be otherwise meaningless. For energy harvesting, as in [17], however, the separation between the cells, as shown in [17] and in this paper, has the desirable effect of decreasing the input impedance of each cell through mutual capacitive and inductive coupling.

In [24], we showed that two-dimensional metamaterial arrays can be stacked vertically (to create three-dimensional array) achieving even significantly higher energy conversion efficiency than two-

dimensional arrays. In this work, we study the power efficiency of electrically-small resonators arrays, particularly SRRs. We highlight the importance of cell stacking in achieving good impedance match, thus better energy reception. We present a comparative case study using numerical simulation where a 3×3 patch antenna array is compared to a 9×9 SRR array, both placed on the same platform. An experiment is provided purely to demonstrate the improvement in efficiency the metamaterial array can provide in comparison to the classical microstrip patch antenna.

We like to emphasize from the outset that this work did not present any optimization of neither the use of microstrip patch antennas that populate a specific footprint (used here for comparison) nor the relative distance and orientation of the SRR cells in the case of the metamaterial. Based on our experience thus far, we believe that optimization can lead to even higher energy harvesting efficiencies; an investigation that we hope to attempt in the near future.

2. CRITICAL CONSIDERATIONS AND BUILDING BLOCKS OF RECTENNA SYSTEMS

A general structure of a basic WPT system is shown in Figure 1 which consists of three main subsystems: a transmitter, a travelling medium (i.e., free space), and a receiver. The function of the first block, which represents a transmitter, is to convert DC power to microwaves using a transmitting circuit and a transmitting antenna. These microwaves will radiate through the transmitting antenna and travel across free space towards a receiver, represented by the third block. The receiver, which represents a rectenna system, converts microwave power to AC power using a receiving antenna. The captured AC power is then converted to DC using a rectifying circuit.

In the receiving system (designated as the Receiving Antenna and Receiver in Figure 1), there are five primary blocks which form a rectenna system as shown in Figure 2. The electromagnetic energy is captured using a receiving antenna operating at a desired frequency. An RF filter is used to suppress unwanted harmonics arising from the nonlinear behaviour of the diode. After the AC power channels from the antenna through the RF filter, a Schottky diode is used to rectify or convert the collected AC power to DC. An additional low-pass filter is connected after the diode for eliminating any remaining AC components.

In previous works, the energy collector elements used were classical antennas of printed (low-profile) [13–16, 25, 26], and non-printed types [8]. Interestingly, in all previous works concerned with electromagnetic power transfer or electromagnetic energy harvesting, the antennas used were those that have been tested and employed extensively for communication systems. In electromagnetic energy harvesting, antennas are used purely in the receiving mode. Despite the applicability of the reciprocity theorem to receive-transmit antenna pair, a receiving antenna's behavior cannot be comprehensively predicted by understanding its behavior when operating in the transmission mode. These, amongst other considerations particular to reception of traveling plane waves, design of receiving antennas or energy collectors in general needs to be viewed with a fresh perspective distinct from that considered



Figure 1. Functional blocks of a typical Wireless Power Transfer (WPT) system.

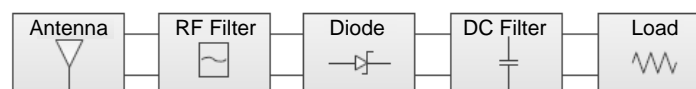


Figure 2. A block diagram for a generic rectenna system using an antenna as the primary collector.

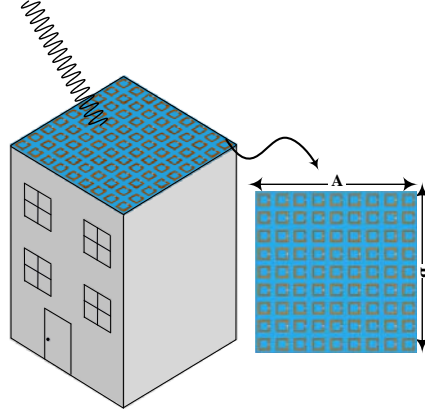


Figure 3. An illustration describing the proposed efficiency concept and highlighting the importance of the total footprint in the overall consideration of the energy-harvesting system.

for communication systems.

We demonstrated through numerical simulation and experiment that an SRR array can be used to collect electromagnetic energy [17]. In developing a new electromagnetic energy harvesting platform, it is critical to demonstrate that the new platform, for now assumed to be a flat surface, provides energy conversion efficiency higher than what could have been achieved using previously used collector or antenna technology. Notice that in general, the efficiency of an antenna in the transmission mode is different from that in the receiving mode. In the transmission mode, the efficiency of the antenna is simply the ratio of the power radiated to the power accepted by the terminals of the antenna. In the receiving mode, the antenna experiences a plane wave arriving from one or more directions, a physical scenario that is not reciprocal to the energy *explosion* scenario of the transmission mode (Notice that an implosion of waves would be the reciprocal of the explosion of waves, which is clearly not what the receiving antenna experiences). Therefore, a new method for computing the efficiency of collectors is introduced for describing the efficiency of collectors in general and their ability to harvest the available electromagnetic energy. For example, if a rooftop of a building of defined area $A \times B$ as shown in Figure 3 is to be used for electromagnetic energy harvesting then the efficiency of the system would be the efficiency of the collectors to convert all power incident on the rooftop to available AC power. It is important to realize that this new definition, first reported in [17], does not depend on the effective area of the collectors but on the total area occupied by the collectors. This definition is given by

$$\eta = \frac{P_{av}}{P_{area}} \quad (1)$$

where P_{area} is the total time-average power incident on the footprint and P_{av} is the time-average AC power received by all collectors occupying the same footprint under consideration and which is available at the feed terminal of the receiving collectors. For N collectors, P_{av} is given by:

$$P_{av} = \sum_{i=1}^N \frac{V_i^2}{R_i} \quad (2)$$

where V_i is the voltage across and the resistance R_i of collector i . This efficiency definition allows for a meaningful comparison between different energy collectors.

In this work, we extend the preliminary study reported in [17] and demonstrate the efficacy of the SRR array for energy harvesting in comparison to an optimized array of microstrip patch antennas occupying identical footprint to that occupied by the SRR array. We emphasize, nevertheless, that this work is focused foremost on demonstrating the viability of SRR array for energy harvesting, namely the conversion of the incident field to AC power available at the feed of the collectors by employing a resistive termination at the gap of the SRR. Furthermore, we study the performance of several optimized structures while highlighting the importance of inter-element coupling in tuning the input impedance of

each cell collector. The rectification system of choice can be applied to either systems without changing the conclusions achieved here.

3. ENERGY HARVESTING USING METAMATERIALS

Metamaterials are typically formed by assembling electrically small resonators that take various shapes and compositions [27]. One of the most common type of resonators is the SRR which is made of single, multiple, concentric or parallel electrically small broken rings [28, 29]. The fact that an SRR develops a relatively high electric field within its structure at resonance frequency, which implies a build up of a voltage across its gap, is indicative of its ability to harvest electromagnetic energy. A single broken loop, such as an SRR element, can be realized as a simple RLC circuit where the dimensions directly affect the overall inductance and capacitance of the SRR. Hence, by varying these dimensions, one can design an SRR to resonate at a specific frequency. At the resonant frequency, the SRR exhibits a concentration of electromagnetic energy where the magnetic field is significantly more dominant than the electric field. A detailed study of the effect of varying the mentioned parameters on the SRR resonance frequency can be found in [30, 31].

When an SRR is excited by a magnetic field normal to the plane of the SRR, a highly concentrated electric field develops across the gap of the structure, as indicated by the red color in Figure 4 for a single ring SRR. Even if the incident field is incident at an angle to the normal, resonance can be excited in the SRR leading to a concentration of electric field across the gap. Since the gap is electrically small, we can interpret the field buildup across the gap as a voltage. Effectively, the field-illuminated SRR becomes a voltage source.

An SRR cell was designed using the full-wave simulator ANSYS HFSS to resonate at around 5.8 GHz. The designed SRR has dimensions of $l = 5.9$ mm, $w = 0.55$ mm and $g = 0.8$ mm as shown in

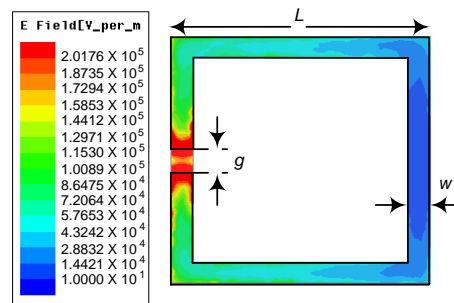


Figure 4. The distribution of the electric field on the plane of a single ring SRR, where the dark red color indicates high energy concentration in the gap of the SRR.

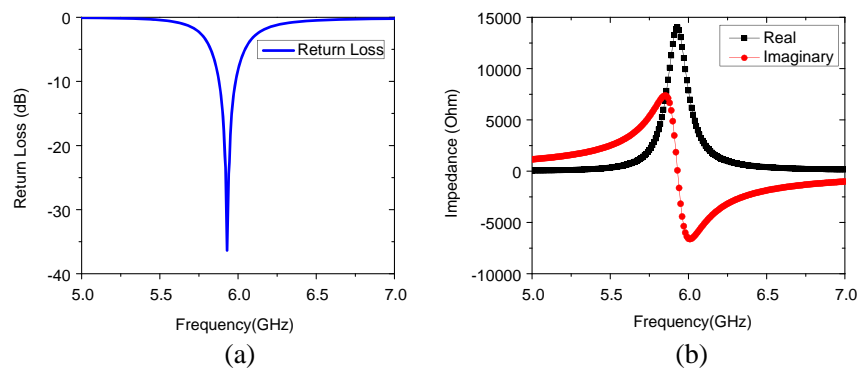


Figure 5. (a) Simulated reflection coefficient of a single SRR. (b) Simulated real and imaginary part of the input impedance of a single SRR fed by a voltage source at the gap.

Figure 4. Since the optimal resistance value is not known in advance, the input impedance at the gap of the SRR needs to be computed. To this end, the SRR was excited by a source placed at the gap of the resonator. The input impedance of the resonator was extracted for a range of frequencies as shown in Figure 5. From Figure 5(b), the impedance seen at the gap of the SRR at the resonance frequency is purely resistive with a value of $14\text{ k}\Omega$. The SRR was then loaded with a resistor and excited by a plane wave such that the magnetic field is perpendicular to the SRR plane. It was found that maximum power dissipation across the resistive load occurs for a resistance value of $14\text{ k}\Omega$. This confirms that maximum power absorption occurs when the load is equal to the input resistance of the SRR. In the case of an SRR array, however, the mutual coupling between the cells significantly affects the input impedance of each SRR cell and consequently the optimal resistance for maximum power absorption also changes. Another factor that affects mutual coupling is the relative orientation of the SRR cells. In [32], it was shown that the orientation indeed affects the overall efficiency. However, optimization of the overall efficiency with respect to the relative orientation of the SRR cells and their relative spacing is deferred to future work. In fact, in light of the input impedance analysis performed here, the resistance used in [17] could not have been optimal (for receiving maximum power) in any sense.

4. SRR ARRAY VS. PATCH ANTENNA ARRAY

Considering the efficiency definition introduced in [17], a demonstration is presented comparing the efficiency of an array of SRRs with an array of patch antennas, both placed on the same footprint as shown in Figure 6. The array of SRRs contained 81 SRR elements, all of identical size and designed to resonate at around 5.85 GHz . An array of 3×3 identical patch antennas was placed on the same footprint, each resonating at the same frequency of 5.85 GHz . Both the SRR array and the patch antenna array were placed on top of a Rogers RT/duroid 5880 substrate having a dielectric constant of $\epsilon_r = 2.2$, loss tangent of 0.0009 and substrate thickness of $t = 0.787\text{ mm}$. The total footprint area was $85 \times 85\text{ mm}^2$.

To ensure that the footprint is utilized efficiently by the patch antennas, the maximum number of antennas that can be placed on the defined footprint and is able to deliver maximum power to the loads is studied. In other words, how many antennas can be placed on the defined footprint so that the sum of the power developed across each load is maximum. In addition, each antenna must be terminated by a load that is equal to the input impedance of the patch antenna to ensure maximum power delivery to each load. Therefore, two essential numerical experiments were conducted.

First a patch antenna operating in the receiving mode was designed to resonate at around 5.8 GHz . The patch antenna has dimensions of width $x = 12\text{ mm}$ and length $y = 14.8\text{ mm}$ as shown in Figure 6. The patch was excited by a horn antenna placed a distance of 120 cm away from it to ensure a plane

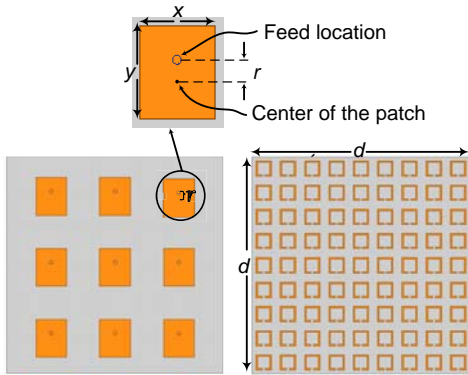


Figure 6. A 9×9 SRR array and a 3×3 patch antenna array occupying the same footprint.

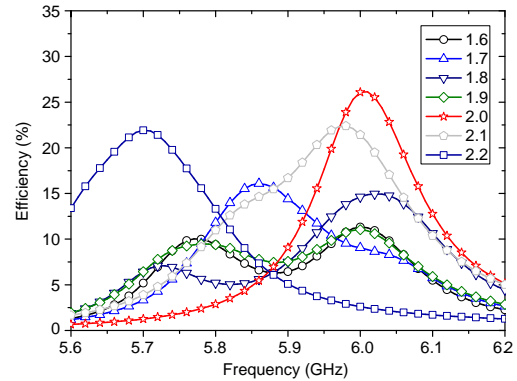


Figure 7. The efficiency of the patch antenna with different coax position (r) with reference to Figure 6.

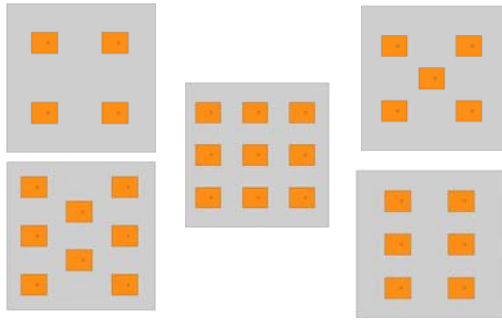


Figure 8. Various patch antenna array configurations.

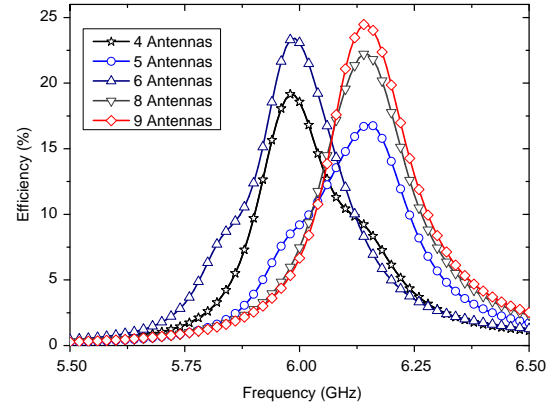


Figure 9. Energy harvesting efficiency of 4, 5, 6, 8, and 9 antenna array.

wave excitation in close proximity of the patch antenna. The patch antenna was terminated by a coaxial line having an input impedance of 50Ω . The performance of a probe-fed patch antenna in terms of power collection efficiency is strongly dependent on the feed position. Hence, the feed position was analysed by varying the location of the coax with a distance r (see Figure 6). Figure 7 shows that the best performance of an isolated patch antenna was achieved when the probe was placed a distance of 2 mm away from the center of the antenna. Therefore, the optimal coax probe feed position was selected for all the patch antennas populating the footprint.

The second numerical experiment studies the maximum number (N) of antennas that can be placed on the defined footprint in such away that the total power collected by the N antennas is maximum. We emphasize that our choice for the feed location for the patch antennas and the number of antennas was selected by inspecting a number of possible solutions with the goal of maximizing power collection across the loads of the antennas and then the best case was chosen. When antennas are placed in close proximity to each other, they interact, introducing mutual coupling, which in turn changes the current in the antenna from that if the antenna was isolated in free space. Mutual coupling changes the input impedance of the antennas and can affect their efficiency in both the receiving and transmitting modes [33]. Typically, antennas need to be separated by approximately at least $1/2$ of the free-space wavelength to retain their independent characteristics such as efficiency, radiation pattern and gain [34]. Five different configurations were studied to achieve maximum power reception. The possible configurations were limited by an a priori specified footprint. In each case, the antennas were placed in such a way that the distance between two adjacent antennas was maximized to reduce coupling and to achieve maximum power collection by each antenna. The five cases are shown in Figure 8. The number of antennas were varied between 4 and 9. It was found through numerical simulation that the antenna configuration containing 9 antennas (see Figure 9) resulted in the maximum power efficiency, and therefore was selected for comparison with the SRR array. Different from patch antennas, the coupling among SRR cells is very critical to the total amount of power absorbed by the SRR array. In addition, the distance between two adjacent SRRs indicated by the separation s in Figure 15 plays a key role in controlling the input impedance of each SRR. This can be clearly understood by comparing the input impedance of a single SRR ($14\text{ k}\Omega$) and an array of SRRs (150Ω) as shown in Figure 5(b) and Figure 15 respectively. Therefore, the SRRs were densely stacked in the available footprint to maximize the absorbed power.

The efficiency performance of the 3×3 antenna array is compared to a 9×9 SRR array. The SRR array was made of SRR cells having the same dimensions as discussed above and with cell spacing of 3.5 mm. For this particular spacing and total number of cells, a load resistance of $2.1\text{ k}\Omega$ gave maximum efficiency. Each array is excited by a horn antenna placed a distance of 120 cm away from the array to ensure that a plane wave is incident on the array (this type of excitation is the basis used for all the array simulations discussed in this section). The SRR receives maximum power when the H -field is normal to the plane of the SRR which is not the case for the patch antenna. Therefore, for a fair

comparison, three tests were conducted for each array with incident field angles of 30° , 45° , and 60° (see Figure 10 for the incident angle definition). The angle ϕ is measured with respect to the x -axis, as indicated in Figure 10. Figures 11, 12, and 13 show the efficiency of the antenna array and the SRR array for incidence angles of 30° , 45° , and 60° , respectively. Table 1 summarizes the numerical simulation results. In the table, the bandwidth was calculated by considering the range of frequencies where the efficiency exceeds 40% and 10% for the SRR array and antenna array, respectively.

From the results obtained the following observations can be drawn:

- The SRR array resulted in higher efficiency for all the incident field angles selected.
- The bandwidth of the SRR array is significantly wider than that of the patch antenna array. More specifically, the SRR array resulted in a bandwidth up to 3.10 GHz over which the efficiency exceeds 40% while the antenna array resulted in a bandwidth of only 450 MHz over which the efficiency exceeds 10%.
- For SRRs, the coupling between adjacent elements has a constructive effect of the total bandwidth of the collected power since the bandwidth of a single SRR (Figure 5(a)) is only 200 MHz while the bandwidth of the SRR array has expanded to around 3.10 GHz.

In the above numerical tests, the analysis focused on the AC power developed across the surface-mount resistor placed at the gap of the resonator. In a practical energy harvesting system, this resistor

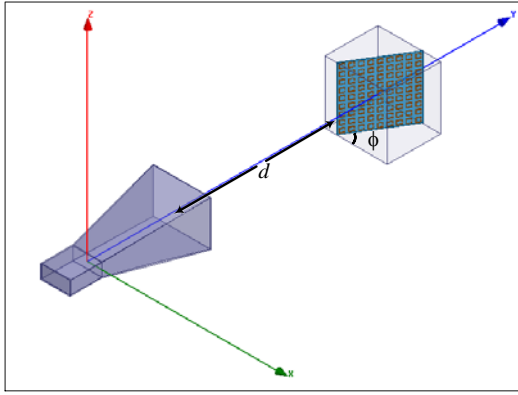


Figure 10. Numerical simulation setup for energy harvesting using a horn antenna as the source of radiation and an SRR array as the collector.

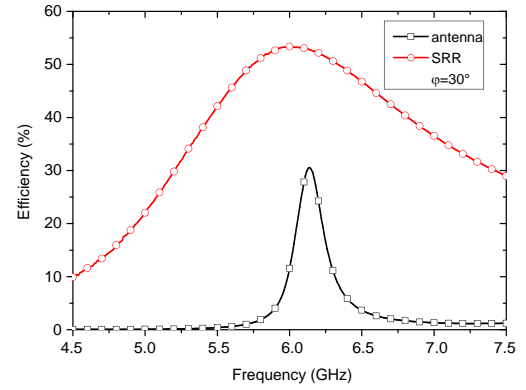


Figure 11. Energy harvesting efficiency of the 9×9 SRR array vs. a 3×3 patch antenna array both tilted at 30° .

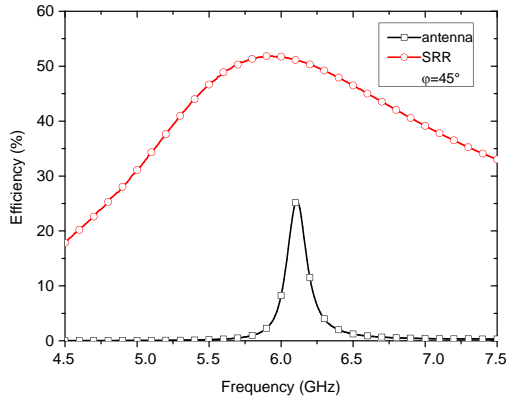


Figure 12. Energy harvesting efficiency of the 9×9 SRR array vs. a 3×3 patch antenna array both tilted at 45° .

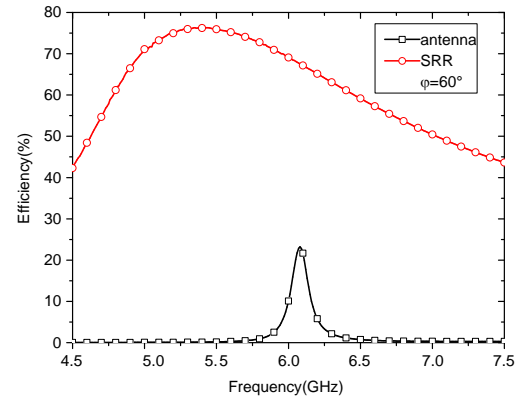


Figure 13. Energy harvesting efficiency of the 9×9 SRR array vs. a 3×3 patch antenna array both tilted at 60° .

is replaced by a full rectification circuitry that is capable of converting AC power to DC employing matching networks, diodes such as Schottky diodes and a load. Designing such rectification circuit depends on the SRR input impedance. The equivalent circuit model of a *receiving* single loop SRR is shown in Figure 14, where R is the total resistance (radiation and Ohmic), L is the self inductance, and C represents the gap capacitance of the SRR. Here, it is assumed that the resonator is operating at resonance frequency while illuminated by an incident electromagnetic field. Notice that we represented the voltage induced within the SRR (which is essentially part of the entire emf voltage induced due to the arriving incident wave) as a dependent voltage source. Whether the dependent voltage source is current dependent or voltage dependent is not of relevance here. What matters is that it is a dependent voltage source that depends on the magnitude, polarization and frequency of the incident electromagnetic field.

In earlier works using SRR as a building block for metamaterial, the gap provided the capacitance needed for resonance. To harvest energy from the SRR through the gap, a resistive load needs to be placed across the gap. The optimal load resistance at the gap that will maximize power absorption depends on the topology of the SRR. Therefore, when designing a loaded SRR to operate at a specific frequency, the load resistance that can achieve maximum power transfer can be found through constrained optimization by varying the resistance and selecting the resistance value that will provide maximum power dissipation across the gap for a particular field polarization and angle of incidence. With reference to Figure 5(b), it is interesting to note that a single square loop with a perimeter of $\lambda_o/2$ experiences high resistance at the resonance frequency. This is due to the fact that at this small loop size, the radiation resistance is much smaller than the case where the perimeter size is slightly larger than a wavelength [35, 36]. However, when we stack the high resistive loops in a way that each loop is in close proximity to adjacent loops, the input impedance is reduced dramatically to values that allow for integration of a practical matching networks and other type of associated circuitries. (Interestingly, the change in the internal impedance of the loops was also observed and accounted for in [37]). In the following section, we show that by stacking a 12×12 SRR loops, one can significantly reduce the input impedance of each cell from $14 \text{ k}\Omega$ (Figure 5(b)) to 150Ω or other desired value by varying the distance among the SRR cells.

5. EXPERIMENTAL VERIFICATION

In this work, the objective is to continue demonstrating the effectiveness of metamaterial arrays for converting the field energy into available AC power. Experimentally validating the precise structure considered above is especially time consuming since the voltage needs to be probed at each SRR gap while sweeping over some range of frequencies. Here, we consider a single patch antenna and compare its energy harvesting performance with an array of SRR cells placed on the same footprint of the patch antenna. The patch antenna and the SRR array were redesigned to operate at 3 GHz. (Our choice of 3 GHz was purely due to the constraints of available test equipment). First a single square patch antenna with a side $a = 25.1 \text{ mm}$ was designed to resonate at 3 GHz as shown in Figure 15. The patch antenna was placed on top of a grounded RO4350 substrate having a thickness of $t = 1.524 \text{ mm}$, a dielectric constant of $\epsilon_r = 3.66$ and a footprint area of $60 \times 60 \text{ mm}^2$. Then the same footprint was used to populate an array of 12×12 SRRs with each cell having dimensions of $l = 4.7 \text{ mm}$, $w = 0.6 \text{ mm}$ and $g = 0.5 \text{ mm}$

Table 1. The performance of the SRR array as compared to the antenna array.

<i>Collector Type</i>	<i>Incident Angle</i>	<i>Max Efficency (%)</i>	<i>Bandwidth (GHz)</i>
SRR Array	30°	53.37	1.40
	45°	51.84	1.65
	60°	76.31	3.10
Antenna Array	30°	30.56	0.45
	45°	25.52	0.25
	60°	23.21	0.20

(for SRR dimensions, see Figure 4). The SRRs were separated by a distance of $s = 0.3$ mm as shown in Figure 15. The SRR array was hosted by a 2.54 mm thick TMM10i substrate with a dielectric constant of $\epsilon_r = 9.9$. The substrate type for both the patch antenna and the SRR array was selected to optimize the performance of each structure.

Then the single patch antenna and the SRR array were fabricated and terminated with the matched impedance as shown in Figure 16. A $150\ \Omega$ surface mount resistor was placed across the gap of each SRR cell and $50\ \Omega$ surface mount resistor was placed between a via soldered to the patch and the ground plane.

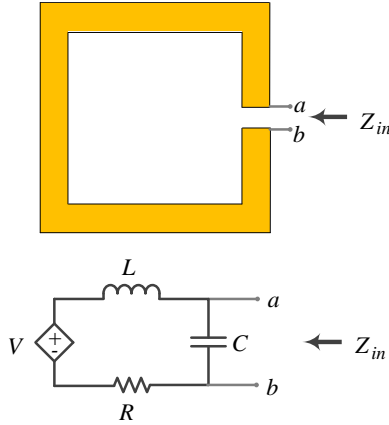


Figure 14. Equivalent circuit model of a single loop SRR.

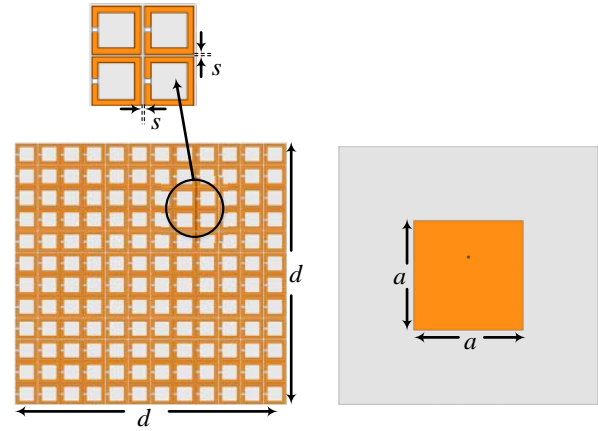


Figure 15. A 12×12 SRR array and a single patch antenna occupying the same footprint.

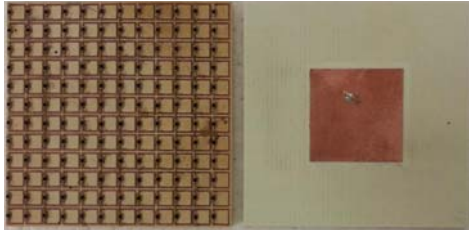


Figure 16. A photo showing the fabricated SRR array and the patch antenna both occupying the same footprint and loaded with the matched resistive load.

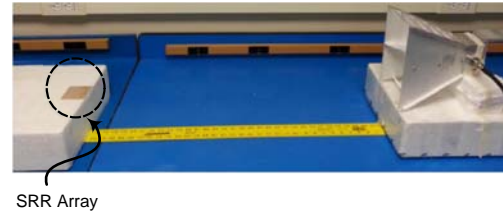


Figure 17. A photo showing the experimental setup used for both the SRR array and the patch antenna.

Table 2. The measured output power captured by the patch antenna and the SRR array.

Collector Type	Frequency (GHz)	Power Received (mW)
SRR Array	2.5	1.16
	2.75	1.29
	2.8	1.28
	3	1.07
Single Patch	2.9	0.43
	3.05	0.76
	3.10	0.74
	3.15	0.34

Using a commercially available 12 dB gain horn antenna, an incident field was generated having a center frequency of 3 GHz. Then the fabricated SRR array was placed a distance of 1 m away from the horn antenna to ensure a plane wave excitation as shown in Figure 17. The SRR array was positioned such that the H -field is normal to the plane of the array. A 4 GHz Rohde and Schwarz RTO Digital Oscilloscopes equipped with a differential probe was used to record the voltage across each resistive load. It was found that the SRR array was able to absorb 1.29 mW of the incident field at 2.75 GHz as shown in Table 2. The power collected by the SRR array in Table 2 was calculated by summing the measured power absorbed across the resistors of all 144 SRR cells at a certain frequency. The slight deviation of the resonance frequency is attributed to fabrication error. Similarly, the patch antenna was excited with the same setup except that the patch antenna was positioned so that the E -field is parallel to the patch surface. It was found that the patch was capable of capturing a maximum power of 0.76 mW as indicated by Table 2. The type of field excitation was chosen such that both structures experience maximum incident field absorption. It is evident from the experimental results that the SRR is capable of absorbing more power per footprint when comparison to the patch antenna. In fact, the results show 70% improvement of the harvested power when using SRRs.

6. DISCUSSION

Since the emergence of metamaterials and until very recently when the potential of harvesting electromagnetic energy using metamaterial particles was first introduced [17], metamaterial has never been analyzed for the reception of electromagnetic energy. In order to understand the feasibility of a single metamaterial cell, especially the SRR, to receive energy in the far field, similar to classical antennas, we revisited the concept of reciprocity.

Reciprocity states that for any two radiating elements in a certain medium, if a 1 Amp current source is placed across the feed nodes of either radiators and the voltage is recorded across the *open* circuit feed of the other radiator, then exchanging the current source and voltmeter produces the same reading (see for example the discussion in [35]). A very simple numerical experiment is conducted to show that even though the SRR is an electrically small resonator, it indeed follows the rules of reciprocity and can therefore receive energy. To this end, we consider a dipole antenna and a single loop SRR, both resonating at the same frequency. The experiment is divided into four cases: for the first case, an SRR is excited by a current source placed across its gap and then the voltage across the feed of the dipole antenna is recorded. In the second case, a dipole antenna is excited by a current source placed at its feed, then the voltage across the gap of the SRR is recorded as shown in Figures 18(a) and (b). The voltage of both cases can be found as $V = \mathbf{E} \cdot \mathbf{d}$ where \mathbf{E} is the electric field at the feed and \mathbf{d} is the gap length vector of the feed of each radiator. Simulation results give identical voltage readings for

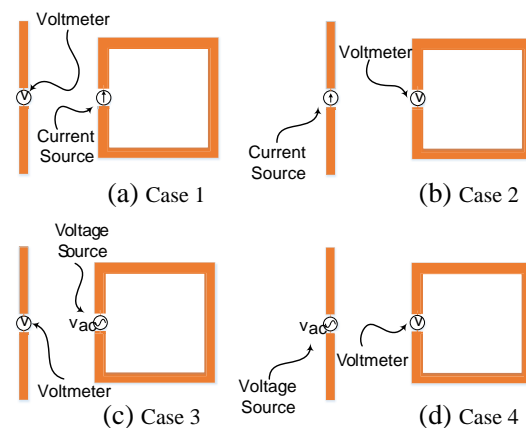


Figure 18. Simulation setup illustrating the reciprocity theorem for (a) case 1, (b) case 2, (c) case 3, and (d) case 4, as described in the Section 6. In each case, the relative size of the two radiators is not to scale.

both cases. When a voltage source was used instead of a current source, as in Figures 18(c) and (d), different readings were obtained for the feed voltages.

These results confirm that despite reciprocity, the potential for an antenna to be an efficient transmitter does not equate to its potential to be an efficient receiver. This very simple numerical exercise shows conclusively that while the SRRs might not be a suitable choice to operate as a transmitting antenna due to practical source considerations, they indeed can operate as a receiver whose effectiveness can be varied due to additional factors such as impedance matching and proximity to adjacent cells.

7. CONCLUSION

The feasibility of using SRRs to harvest microwave energy was studied through simulation by first placing a resistive load across the gap of a single loop SRR then calculating the power dissipated across the resistor. An experiment was then conducted to test the feasibility of SRRs to harvest microwave energy. The fabricated SRR cell was excited by an antenna placed 30 cm away, and then the voltage across the gap was measured using a high-frequency oscilloscope. A voltage of 611 mV was observed across the gap when 24 dBm power level was pumped into the transmitting antenna feed.

The efficiency of an array of SRRs was compared to that of an array of antennas occupying the same footprint. The numerical simulation results show that the SRR array is capable of electromagnetic energy harvesting efficiency of 40% or higher over a bandwidth of 3.10 GHz while the patch antenna array gave an efficiency of 10% or higher over a bandwidth of only 450 MHz. While we provided comparison to an array of patch microstrip antennas, other types of patch antennas could provide lower or possibly higher efficiency than the microstrip antenna array used here. It is evident from the numerical simulations presented that the SRR array provides significantly higher power harvesting efficiency and more critically wider bandwidth as compared to the antenna array. As a proof of concept, a single patch antenna and a 12×12 SRR array were compared in terms of maximum power output captured by each structure. It was found that the SRR array provided 60% more power per footprint than the patch antenna which verify the results obtained through numerical simulation. These results are expected to have strong impact on the viability and efficiency of electromagnetic energy harvesting in general.

ACKNOWLEDGMENT

The authors like to acknowledge the support of the Natural Sciences and Engineering Research Council, Canada and the Saudi Arabian Ministry of Higher Education. We also would like to acknowledge CMC Microsystems for the provision of products and services that facilitated this research, including CAD tools and test support.

REFERENCES

1. Brown, W. C., "The history of power transmission by radio waves," *IEEE Transactions on Microwave Theory and Techniques*, Vol. 32, No. 9, 1230–1242, 1984.
2. Curty, J., M. Declercq, C. Dehollain, and N. Joehl, *Design and Optimization of Passive UHF RFID Systems*, Springer Publishing Company, Incorporated, 2010.
3. Yagi, H. and S. Uda, "On the feasibility of power transmission by electric waves," *Proceedings of the Third Pan-Pacific Science Congress*, Vol. 2, 1305–1313, 1926.
4. "Electric light without current," *Literary Digest*, Vol. 112, 30, 1932.
5. Strassner, II, B. and K. Chang, "Rectifying antennas (rectennas)," *Encyclopedia of RF and Microwave Engineering*, 2005.
6. Erb, R., "Power from space — The tough questions: The 1995 Peter E. Glaser lecture," *Acta Astronautica*, Vol. 38, No. 48, 539–550, 1996, Benets of Space for Humanity, Online Available: <http://www.sciencedirect.com/science/article/pii/0094576596823241>.

7. Glaser, P. E., "An overview of the solar power satellite option," *IEEE Transactions on Microwave Theory and Techniques*, Vol. 40, No. 6, 1230–1238, 1992.
8. Brown, W., "Electronic and mechanical improvement of the receiving terminal of a free-space microwave power transmission system," *NASA STI/Recon Technical Report N*, Vol. 77, 31613, 1977.
9. McSpadden, J., "Rectifying and oscillating integrated antennas," Ph.D. Dissertation, Texas A&M University, 1998.
10. Brown, W. and J. Triner, "Experimental thin-film, etched-circuit rectenna," *1982 IEEE MTT-S International Microwave Symposium Digest*, 185–187, 1982.
11. Koert, P., J. Cha, and M. Machina, "35 and 94 GHz rectifying antenna systems," *SPS 91 — Power from Space*, Vol. 1, 541–547, 1991.
12. Bharj, S., R. Camisa, S. Grober, F. Wozniak, and E. Pendleton, "High efficiency C-band 1000 element rectenna array for microwave powered applications," *1992 IEEE MTT-S International Microwave Symposium Digest*, 301–303, 1992.
13. Ren, Y. and K. Chang, "5.8-GHz circularly polarized dual-diode rectenna and rectenna array for microwave power transmission," *IEEE Transactions on Microwave Theory and Techniques*, Vol. 54, No. 4, 1495–1502, 2006.
14. Harouni, Z., L. Cirio, L. Osman, A. Gharsallah, and O. Picon, "A dual circularly polarized 2.45 GHz rectenna for wireless power transmission," *IEEE Antennas and Wireless Propagation Letters*, Vol. 10, 306–309, 2011.
15. Hagerty, J. and Z. Popovic, "An experimental and theoretical characterization of a broadband arbitrarily-polarized rectenna array," *2001 IEEE MTT-S International Microwave Symposium Digest*, Vol. 3, 1855–1858, 2001.
16. Hagerty, J., F. Helmbrecht, W. McCalpin, R. Zane, and Z. Popovic, "Recycling ambient microwave energy with broad-band rectenna arrays," *IEEE Transactions on Microwave Theory and Techniques*, Vol. 52, No. 3, 1014–1024, 2004.
17. Ramahi, O., T. Almoneef, M. Alshareef, and M. Boybay, "Metamaterial particles for electromagnetic energy harvesting," *Applied Physics Letters*, Vol. 101, No. 17, 173903, 2012.
18. Yoo, T. and K. Chang, "Theoretical and experimental development of 10 and 35 GHz rectennas," *IEEE Transactions on Microwave Theory and Techniques*, Vol. 40, No. 6, 1259–1266, 1992.
19. McSpadden, J., L. Fan, and K. Chang, "A high conversion efficiency 5.8 GHz rectenna," *1997 IEEE MTT-S International Microwave Symposium Digest*, Vol. 2, 547–550, 1997.
20. Chin, C., Q. Xue, and C. Chan, "Design of a 5.8-GHz rectenna incorporating a new patch antenna," *IEEE Antennas and Wireless Propagation Letters*, Vol. 4, 175–178, 2005.
21. Strassner, B. and K. Chang, "5.8-GHz circularly polarized rectifying antenna for wireless microwave power transmission," *IEEE Transactions on Microwave Theory and Techniques*, Vol. 50, No. 8, 1870–1876, 2002.
22. Monti, G., L. Tarricone, and M. Spartano, "X-band planar rectenna," *IEEE Antennas and Wireless Propagation Letters*, Vol. 10, 1116–1119, 2011.
23. Hawkes, A. M., A. R. Katko, and S. A. Cummer, "A microwave metamaterial with integrated power harvesting functionality," *Applied Physics Letters*, Vol. 103, No. 16, 2013, Online Available: <http://scitation.aip.org/content/aip/journal/apl/103/16/10.1063/1.4824473>.
24. Almoneef, T. and O. M. Ramahi, "A 3-dimensional stacked metamaterial arrays for electromagnetic energy harvesting," *Progress In Electromagnetics Research*, Vol. 146, 109–115, 2014.
25. Yo, T., C. Lee, C. Hsu, and C. Luo, "Compact circularly polarized rectenna with unbalanced circular slots," *IEEE Transactions on Antennas and Propagation*, Vol. 56, No. 3, 882–886, 2008.
26. Heikkinen, J. and M. Kivikoski, "A novel dual-frequency circularly polarized rectenna," *IEEE Antennas and Wireless Propagation Letters*, Vol. 2, 330–333, 2003.
27. Solymar, L. and E. Shamonina, *Waves in Metamaterials*, Oxford University Press, USA, 2009.
28. Mei, Z., J. Bai, T. Niu, and T. Cui, "A half Maxwell fish-eye lens antenna based on gradient-index metamaterials," *IEEE Transactions on Antennas and Propagation*, Vol. 60, No. 1, 398–401, 2012.

29. Khan, M. and M. Mughal, "Design of tunable metamaterials by varying the height of rings of S-shaped resonator," *IEEE Third International Conference on Electrical Engineering, ICEE'09*, 1–4, 2009.
30. Aydin, K., I. Bulu, K. Guven, M. Kafesaki, C. Soukoulis, and E. Ozbay, "Investigation of magnetic resonances for different split-ring resonator parameters and designs," *New Journal of Physics*, Vol. 7, 168, 2005.
31. Bilotti, F., A. Toscano, L. Vegni, K. Aydin, K. Alici, and E. Ozbay, "Equivalent-circuit models for the design of metamaterials based on artificial magnetic inclusions," *IEEE Transactions on Microwave Theory and Techniques*, Vol. 55, No. 12, 2865–2873, 2007.
32. AlShareef, M. R. and O. M. Ramahi, "Electrically small resonators for energy harvesting in the infrared regime," *Journal of Applied Physics*, Vol. 114, No. 22, 2013, Online Available: <http://scitation.aip.org/content/aip/journal/jap/114/22/10.1063/1.4846076>.
33. Stutzman, W. L. and G. Thiele, *Antenna Theory and Design*, John Wiley, New York, 1981.
34. Lau, B. K. and Z. Ying, "Antenna design challenges and solutions for compact MIMO terminals," *2011 International Workshop on Antenna Technology (iWAT)*, 70–73, 2011.
35. Balanis, C. A., *Antenna Theory: Analysis and Design*, John Wiley & Sons, 2012.
36. Storer, J. E., "Impedance of thin-wire loop antennas," *Transactions of the American Institute of Electrical Engineers, Part I: Communication and Electronics*, Vol. 75, No. 5, 606–619, Nov. 1956.
37. Gorkunov, M., M. Lapine, E. Shamonina, and K. H. Ringhofer, "Effective magnetic properties of a composite material with circular conductive elements," *Eur. Phys. J. B*, Vol. 28, 263–269, 2002.